Nanochem Res 4(2): 140-147, Summer and Autumn 2019

RESEARCH PAPER

Eco-friendly synthesis and characterization of α-Fe_2O_3 nanoparticles and study of their photocatalytic activity for degradation of Congo red dye

Saeid Taghavi Fardood[1,2,*], Farzaneh Moradnia[1,2], Sajjad Moradi[1], Reza Forootan[1], Fateme Yekke Zare[1], Maryam Heidari[1]

[1] *Department of Chemistry, University of Zanjan, Zanjan, Iran*

[2] *Kordestan Cement Company, Bijar, Kordestan, Iran*

ARTICLE INFO

Article History:
Received 18 March 2019
Accepted 04 September 2019
Published 15 October 2019

Keywords:
α-Fe_2O_3 nanoparticles
Green Synthesis
Arabic Gum
Dye degradation

ABSTRACT

In this work, α-Fe_2O_3 (hematite) nanoparticles were synthesized using Arabic gum (AG) as a biotemplate source by the sol-gel method. This method has many advantages such as low-cost, nontoxicity, simple work-up, high efficiency, compounds uniformity, and high efficiency. The α-Fe_2O_3 nanoparticles were characterized by Fourier transform infrared (FT-IR) spectroscopy, X-ray diffraction (XRD), UV-visible diffuse reflectance spectroscopy (DRS), field emission scanning electron microscopy (FESEM), and transmission electron microscopy (TEM). The results of XRD analysis revealed the formation of the rhombohedral phase of α-Fe_2O_3 nanoparticles with an average crystallite size of 19 nm. The TEM image illustrated the α-Fe_2O_3 nanoparticles with average particle size of 45-50 nm. The application of α-Fe_2O_3 nanoparticles as a photocatalyst was investigated for the degradation of the Congo red dye. The effects of photocatalyst dosage, initial dye concentration and visible light irradiation on dye degradation were assessed. The results demonstrated that the catalyst could degrade 90% of the Congo red dye in 90 min. The α-Fe_2O_3 nanoparticles exhibited slight decrease in photocatalytic degradation of Congo red dye after four recycles.

How to cite this article
Taghavi Fardood S, Moradnia F, Moradi S, Forootan R, Yekke Zare F, Heidari M. Eco-friendly synthesis and characterization of α-Fe_2O_3 nanoparticles and study of their photocatalytic activity for degradation of Congo red dye. Nanochem Res, 2019; 4(2):140-147. DOI: 10.22036/ncr.2019.02.005

INTRODUCTION

Metal oxide nanomaterials are a varied category of materials that have a wide range of applications such as water purification, environmental remediation, energy, personal care products, and medical technology [1-7]. This category of materials, due to their wide band gap and high photosensitive nature, can be used as a photocatalyst for the photocatalytic degradation of organic dyes [8-11].

There are various kinds of iron oxide including hematite (α-Fe_2O_3), maghemite (c-Fe_2O_3) and wustite (FeO) [12, 13], among which α-Fe_2O_3 has features such as band gap 2.1 eV [14], non-toxicity, being cheap, and good chemical stability in aqueous solutions [15, 16]. Also, it has varied applications in water splitting, cement industry, gas sensing, solar energy conversion, lithium-ion battery production, water purification, and pigmentation which all of these have caused increasing attention to the production of these nanoparticles [17-19]. Up to now, several synthetic methods have been developed to produce the α-Fe_2O_3 nanoparticles, including hydrolysis of iron salt, sol-gel, and hydrothermal synthesis [20-24]. Among these methods, the green sol-gel method supply products with a low cost, simple work-up,

* Corresponding Author Email: *saeidt64@gmail.com*

and high efficiency [25-27]. So, this method can be efficient and appropriate for the synthesis of nanoparticles like Fe_2O_3.

One of the main causes of environmental problems is the effluent of factories, such as textile factories, that are released into the environment. In the world, over 10,000 different colors and pigments are produced that 60–70% of them are synthetic azo dyes used in the textile factories [28-30]. Therefore, enter of synthetic colors like azo dyes in the rivers can cause serious risks for the living organisms such as aquatics, plants and human beings [31]. Hence, over the last few years, the researchers have paid more attention on removing the synthetic dyes from the environment. In this work, the photocatalytic activity of α-Fe_2O_3-NPs has been evaluated for the degradation of Congo red dye in the presence of visible light irradiation. FT-IR, XRD, FESEM, and TEM are the techniques that were used for characterization of α-Fe_2O_3 NPs. The chemical structure of dye is observed in Scheme 1 and characteristics of it are listed in Table 1 [32].

EXPERIMENTAL

Materials

Arabic gum (AG) was obtained from a local health food store. $FeCl_3$, as the iron source, was purchased from daijung (Darmstadt, Korea) and used without further purification. The FT-IR spectra were measured on a Jasco 6300 FT-IR spectrometer (KBr disks). The structural properties of synthesized nanoparticles were investigated by X-ray powder diffraction (XRD) pattern on an X'Pert-PRO advanced diffractometer using Cu (Kα) radiation (wavelength: 1.5406 Å) at 40 kV and 40 mA at room temperature in the range of 2θ from 20° to 80°. The external structure of the sample was determined by a Jasco 6300 FT-IR spectroscopy. The FT-IR spectrum was collected between the wavenumber of 400 and 4000 cm^{-1}. The particle size and morphology of the sample were analyzed by Transmission electron microscopy (Philips CM30) and field emission scanning electron microscopy (Zeiss EVO 18, Germany). The diffuse reflectance UV–Vis spectroscopy (DRS) of the sample was recorded by a UV–Vis spectrophotometer (Shimadzu, UV-2550, Japan) using $BaSO_4$ as a reference.

Synthesis of α-Fe_2O_3 nanoparticles using Arabic gum

At first, in order to prepare an Arabic gel, 0.3 g of the Arabic gum (AG) was dissolved in 40 mL of deionized water and stirred for 120 min at 75°C. $FeCl_3$ solution (2 mmol of $FeCl_3$ in 5 mL of deionized water) was added to the gel. Then, the sample container was put in a sand bath and the temperature of the sand bath was fixed at 75 °C with stirring for 12 h to obtain a black color resin. After that, the dry gel was annealed at 600°C for 4 h to obtain a black powder of α-Fe_2O_3.

Photocatalytic dye degradation

Dye degradation experiments were carried out in a batch mode photoreactor. The irradiation source was a fluorescent lamp (λ >400 nm, 80 W, Pars, Iran) installed above the batch photoreactor.

The photocatalytic degradation of Congo red (CR) dye was carried out by various dosages of the sample (0.03, 0.04, 0.05 and 0.06 g) in 50 mL solution of dye (20 mg/L) at room temperature. The effect of initial dye concentration on the photocatalytic dye degradation was studied. For this purpose, 0.05 g of α-Fe_2O_3 was added to 50 mL of different dye concentrations (10, 20, 30 and 40 mg/L). The solute on samples was withdrawn from the reaction medium at regular time intervals. The catalyst was

Table 1. The characteristics of Congo red (CR) dye

Synonym:	Congo red
Molecular formula:	$C_{32}H_{22}N_6Na_2O_6S_2$
Molecular Weight:	696.66 g/mol
λ_{max} :	499 nm
CAS Number:	573-58-0

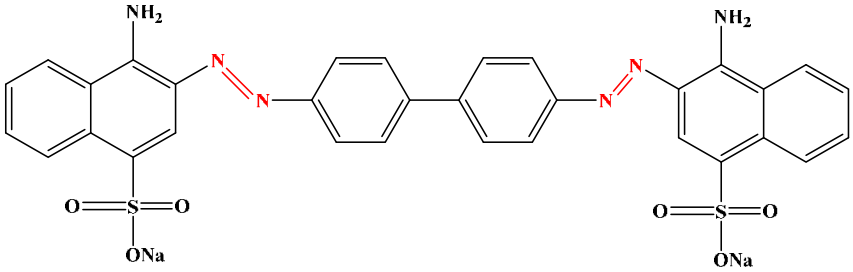

Scheme 1. Molecular structure of Congo red dye

separated from the solution using a centrifuge. The change of absorbance at a maximum wavelength (λ_{max}= 499 nm) of dye was monitored by UV–Vis spectrophotometer. The effect of visible light irradiation on the removal of dyes was surveyed. The percentage of the photocatalytic degradation of dye checked out by the following equation,

$$\%\ Degradation = \frac{A_0 - A_t}{A_0} \times 100$$

Where A_0 is the initial absorbance and A is the final absorbance, at λ_{max} = 499 nm.

RESULTS AND DISCUSSION

Characterization of α-Fe_2O_3-NPs

The FT-IR spectra were recorded in the solid phase using the KBr pellet technique in the range of 400-4000 cm^{-1}. Fig. 1 shows the FT-IR spectrum of the sample calcined at 600°C for 4 h. The spectrum displays two characteristics broad bands at 437-440 cm^{-1} and 537–541 cm^{-1} corresponding to Fe-O stretching. The highest band at 594 cm^{-1} corresponds to intrinsic stretching vibrations of Fe↔O, and the lowest band at 474 cm^{-1} is related to the bending vibration of O↔Fe↔O [33].

Fig. 2 shows the X-ray diffraction patterns of the sample synthesized by AG and calcined at 600°C for 4 h. As shown in Fig. 2, the characteristic diffraction peaks at 2θ are 24.0, 32.98, 35.54, 40.86, 43.39, 49.51, 54.06, 57.42, 62.35, 63.85, 69.52, 71.89, 75.39, 77.70, and 78.70 which can be assigned to (012), (104), (110), (113), (202), (024), (116), (018), (214), (300), (208), (1010), (220), (306), and (223) planes, respectively. All the diffraction peaks were readily indexed to a pure rhombohedral phase of α-Fe_2O_3 (JCPDS Card no. 72-0469) with a=b =

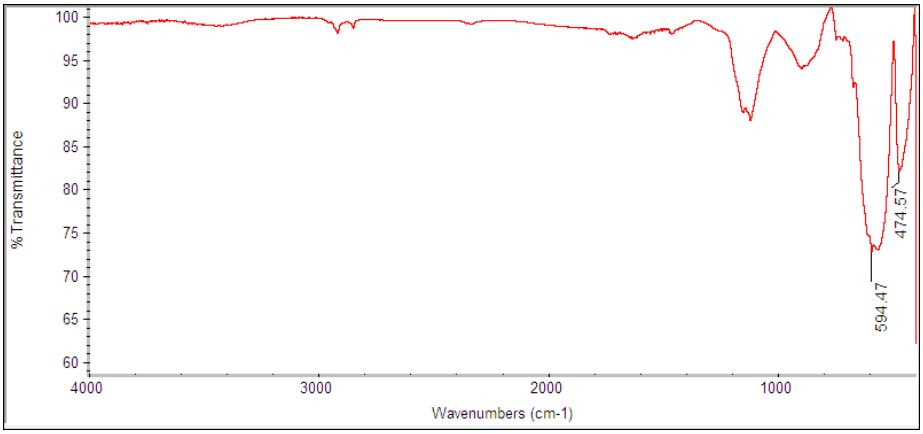

Fig. 1. FT-IR spectrum of α-Fe_2O_3 NPs.

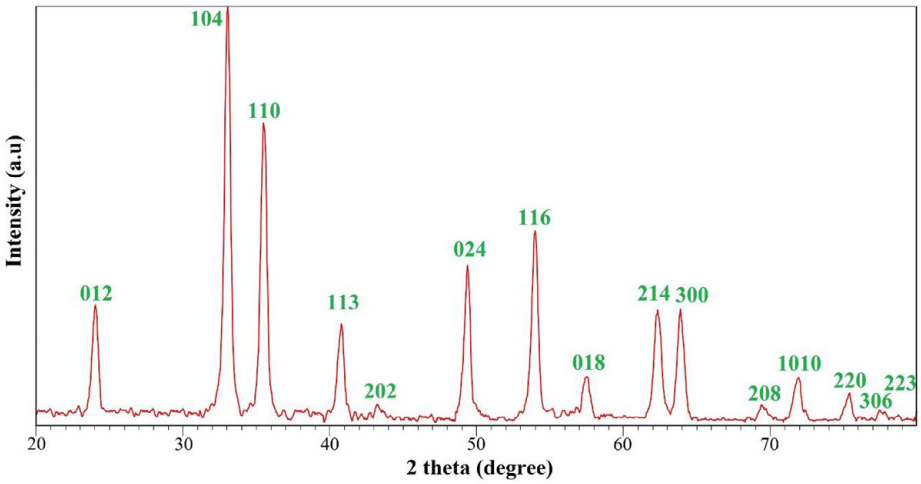

Fig. 2. XRD pattern of α-Fe_2O_3 NPs.

5.041 Å and c = 13.757 Å. The crystallite size of α-Fe_2O_3 NPs was determined from the full width at half maximum (FWHM) of the XRD pattern by the Scherrer formula:

$$D = 0.9\lambda/\beta \cos\theta$$

where D is the crystallite size (nm), λ is the X-ray wavelength of Cu Kα = 0.154 nm, β is the full width at half maximum of the peak, and θ is the Bragg angle [34]. Using the above method we obtained an average size of 19 nm for α-Fe_2O_3 NPs.

The FESEM image shows the particle size and external morphology of the α-Fe_2O_3 NPs (Fig. 3). According to the result of this analysis, nanoparticles of α-Fe_2O_3 produced with this method have a relatively uniform spherical shape in nano-size.

The TEM image in Fig. 4 confirms the morphology and particle size of the α-Fe_2O_3 NPs. As shown in Fig. 4, the α-Fe_2O_3 NPs have spherical morphology and average particle size is about 45-50 nm.

The band gap of *α-Fe_2O_3* nanoparticles was measured by diffuse reflectance spectroscopy (DRS). The band gap energy was calculated by a reflectance technique by exerting the Tauc theory [35]. The results show that the band gap of *α-Fe_2O_3* nanoparticles is roughly 2 eV (Fig. 5). Therefore, it is certified that the *α-Fe_2O_3* nanoparticles are suitable photocatalyst in a visible-light region.

Effect of visible light irradiation and α-Fe_2O_3 NPs catalyst

The photocatalytic activity of *α-Fe_2O_3* NPs on degradation Congo red dye was evaluated under the following state: *α-Fe_2O_3* nano photocatalyst under visible light irradiation, *α-Fe_2O_3* nano

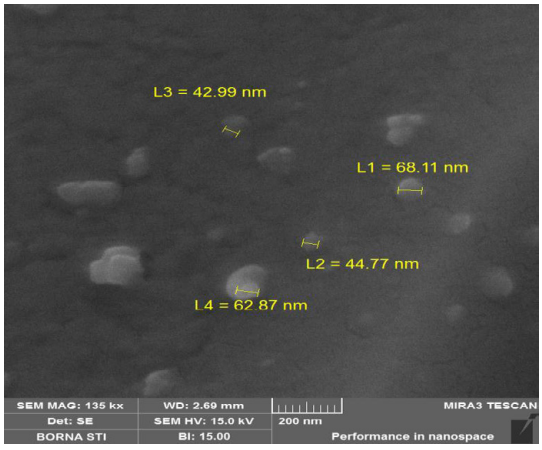

Fig. 3. SEM micrograph of the *α-Fe_2O_3* NPs.

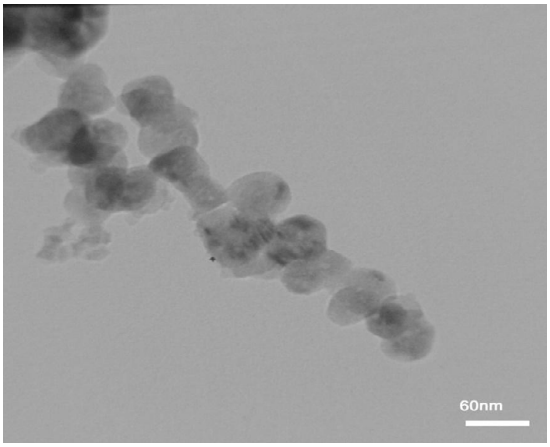

Fig. 4. TEM micrograph of the *α-Fe_2O_3* NPs.

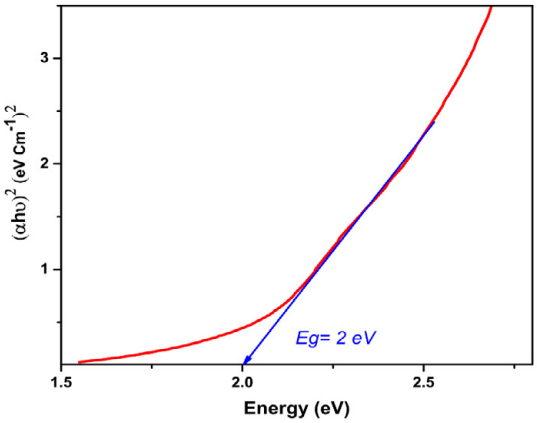

Fig. 5. Tauc plot of the *α-Fe_2O_3* NPs

photocatalyst under dark and visible light irradiation without *α-Fe_2O_3* NPs. As can be seen in Fig. 6, simultaneous applying of α-Fe_2O_3 NPs with visible light irradiation has led to degradation of 90% of Congo red dye within 90 min. When the degradation of dye was followed in the presence of catalyst without visible light, adsorption of dye was attained 45% of Congo red.

The effect of photocatalyst dosage

For checking the effect of the photocatalyst amount on decolorization, the different dosages of α-Fe_2O_3 NPs were used. In this experiment, 0.03- 0.06 gr of the catalyst was applied in 20 mg/L concentration of Congo red and at a constant time of 90 min. Fig. 7 shows the photocatalyst effect of α-Fe_2O_3 dosage on decolorization of dyes percentages for 90 min.

The effect of initial dye concentration

In order to survey the changes of initial dye concentrations on degradation performance, various concentrations between 10 to 40 mg/L were exploited and other operating factors were kept fixed. The relationship between initial dye concentration and degradation efficiency at 0.05 g of the photocatalyst is demonstrated in Fig.8. It was remarked that the rate of photocatalytic degradation decreases as the initial concentration of Congo red dye enhances from 10 to 40 mg/L in 90 min.

The effect of time on the degradation of Congo red dye

The UV-Vis spectra of the Congo red were studied for the following degradation procedure in the presence of α-Fe_2O_3 NPs as the photocatalyst at diverse time gap under the visible irradiation. The maximum absorption peak of C.R is found at 499 nm that clearly decreases in intensity with raising irradiation time (Fig. 9). Approximately 90% of C.R is degraded in 90 min.

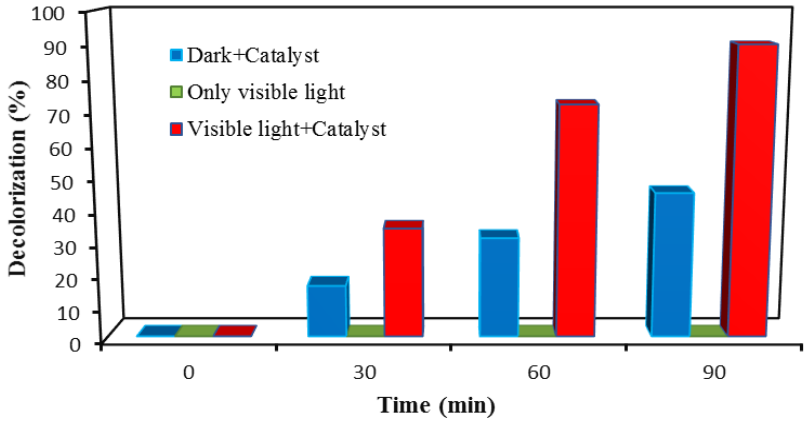

Fig. 6. The effect of visible light irradiation on the decolorization efficiency (%). Reaction conditions: Congo red =20 mg/L, catalyst= 0.05 g, pH=natural and room temperature.

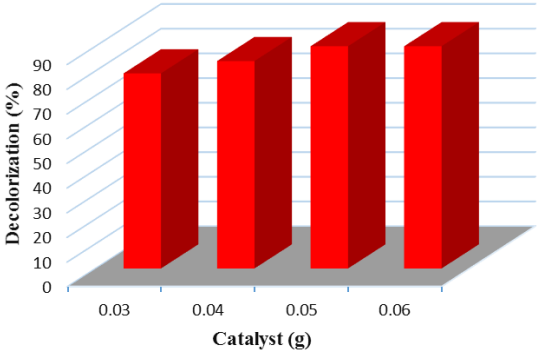

Fig. 7. The effect of photocatalyst dosage on the photocatalytic degradation of Congo red dye (pH = natural, CR=20 mg/L).

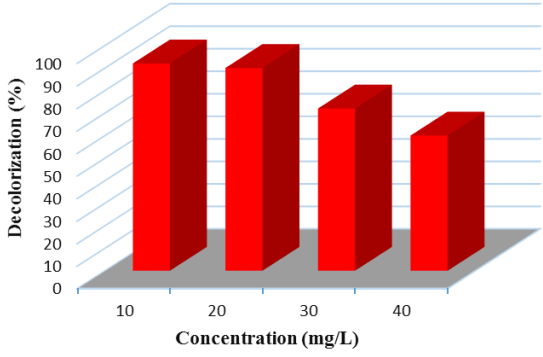

Fig. 8. The effect of the initial concentration of CR dye on the decolorization efficiency (%).

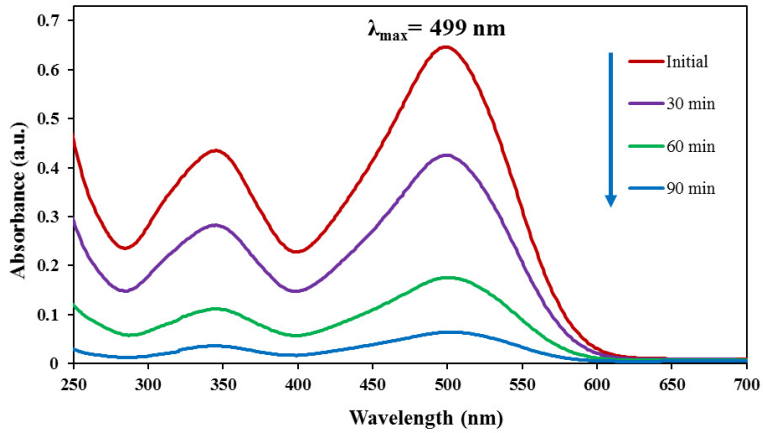

Fig. 9. Absorption spectra of CR solutions (20 mg/L) in the presence of 0.05 g of α-Fe_2O_3 photocatalyst under visible light radiation.

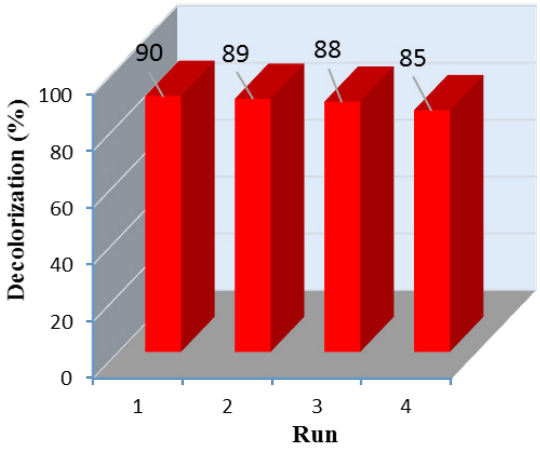

Fig. 10. Recyclability of α-Fe_2O_3NP.

The reusability of the photocatalyst

The reusability of the photocatalyst was measured for the degradation of C.R dye under the determined reaction conditions. In this test, the catalyst was separated from the solution using a centrifuge, and washed with distilled water before using in the subsequent run. As demonstrated in Fig. 10, the nanocatalyst retained usefully and was reused four times with a good degradation performance. So, α-Fe_2O_3 NPs maintain in a good decolorization efficiency and stability.

CONCLUSION

In this work, we have reported the green synthesis of α-Fe_2O_3 NPs using Arabic gum (AG) as a biopolymer template by the sol-gel method. This method has many advantages such as non-toxicity, low cost, simple work-up, compounds uniformity, and high efficiency. The XRD results showed a pure rhombohedral phase after heat treatment at 600°C for only 4 h. Also, the results of FESEM and TEM confirmed the synthesis of nanoparticles with the spherical shape in nanometer size. The photocatalytic activity of the α-Fe_2O_3 nanoparticles was studied for degradation of Congo red dye under visible light irradiation. The results showed that 90% of Congo red dye was degraded within 90 min. The nano-catalyst can be recycled four times with no significant loss of photocatalytic activity.

ACKNOWLEDGMENT

This work was supported by the "*Kordestan Cement Co., Kordestan, Bijar, Iran*" and the "*Atlas Pood Co., Tabriz, Iran*".

CONFLICTS OF INTEREST

The authors declare that they have no conflict of interest.

REFERENCES

1. Cañas-Carrell J, Li S, Parra A, Shrestha B. Metal oxide nanomaterials: health and environmental effects. Health and Environmental Safety of Nanomaterials: Elsevier; 2014. p. 200-21.
2. Saeidian H, Moradnia F. Benign synthesis of N-aryl-3,10-dihydroacridin-1(2H)-one derivatives via ZnO nanoparticle-catalyzed Knoevenagel condensation/ intramolecular enamination reaction. Iranian Chemical Communication. 2017;5(Issue 3, pp. 237-363):252-61.
3. Ramazani A, Moradnia F, Aghahosseini H, Abdolmaleki I. Several Species of Nucleophiles in the Smiles Rearrangement. Current Organic Chemistry. 2017;21(16):1612-25.
4. Taghavi Fardood S, Ramazani A. Black Tea Extract Mediated Green Synthesis of Copper Oxide Nanoparticles. Journal of Applied Chemical Research. 2018; 12(2): 8-15.

5. Ramazani A, Farshadi A, Mahyari A, Sadri F, Joo SW, Asiabi PA, et al. Synthesis of electron-poor N-Vinylimidazole derivatives catalyzed by Silica nanoparticles under solvent-free conditions. International Journal of Nano Dimension. 2016; 7(1): 41.
6. Sadri F, Ramazani A, Ahankar H, Taghavi Fardood S, Azimzadeh Asiabi P, Khoobi M, et al. Aqueous-phase oxidation of alcohols with green oxidants (oxone and hydrogen peroxide) in the presence of $MgFe_2O_4$ magnetic nanoparticles as an efficient and reusable catalyst. Journal of Nanostructures. 2016; 6(4): 264-72.
7. Saeidian H, Mirjafary Z, Abdolmaleki E, Moradnia F. An Expedient Process for the Synthesis of 2-(N-Arylamino) benzaldehydes from 2-Hydroxybenzaldehydes via Smiles Rearrangement. Synlett. 2013;24(16):2127-31.
8. Khayyat SA, Akhtar M, Umar A. ZnO nanocapsules for photocatalytic degradation of thionine. Materials Letters. 2012;81:239-41.
9. Rekavandi N, Malekzadeh A, Ghiasi E. Methyl orange degradation over nano-$LaMnO_3$ as a green catalyst under the mild conditions. Nanochemistry Research. 2019; 4(1): 1-10.
10. Houshmand R, Banna Motejadded Emrooz H. Photocatalytic outcomes for methylene blue degradation from CTAB mediated mesoporous ZnS, synthesized with an insoluble precursor in ethanol media. Nanochemistry Research. 2019; 4(1): 64-76.
11. Singh R, Kumar M, Tashi L, Khajuria H, Sheikh HN. Hydrothermal synthesis of nitrogen doped graphene supported cobalt ferrite (NG@ $CoFe_2O_4$) as photocatalyst for the methylene blue dye degradation. Nanochemistry Research. 2018;3(2):149-59.
12. Zhou H, Wong SS. A facile and mild synthesis of 1-D ZnO, CuO, and α-Fe2O3 nanostructures and nanostructured arrays. Acs Nano. 2008;2(5):944-58.
13. Taghavi Fardood S, Ramazani A, Golfar Z, Joo SW. Green Synthesis of α-Fe_2O_3 (hematite) Nanoparticles using Tragacanth Gel. Journal of Applied Chemical Research. 2017; 11(3): 19-27.
14. Valenzuela M, Bosch P, Jiménez-Becerrill J, Quiroz O, Páez A. Preparation, characterization and photocatalytic activity of ZnO, Fe2O3 and ZnFe2O4. Journal of Photochemistry and photobiology A: Chemistry. 2002;148(1-3):177-82.
15. Kennedy JH, Frese KW. Photooxidation of water at α-Fe2O3 electrodes. Journal of the Electrochemical Society. 1978;125(5):709-14.
16. Lindgren T, Wang H, Beermann N, Vayssieres L, Hagfeldt A, Lindquist S-E. Aqueous photoelectrochemistry of hematite nanorod array. Solar Energy Materials and Solar Cells. 2002;71(2):231-43.
17. Chen J, Xu L, Li W, Gou X. α-Fe2O3 nanotubes in gas sensor and lithium-ion battery applications. Advanced Materials. 2005;17(5):582-6.
18. Gondal MA, Hameed A, Yamani Z, Suwaiyan A. Laser induced photo-catalytic oxidation/splitting of water over α-Fe2O3, WO3, TiO2 and NiO catalysts: activity comparison. Chemical Physics Letters. 2004;385(1-2):111-5.
19. Ohmori T, Takahashi H, Mametsuka H, Suzuki E. Photocatalytic oxygen evolution on α-Fe2O3 films using Fe3+ ion as a sacrificial oxidizing agent. Physical Chemistry Chemical Physics. 2000;2(15):3519-22.
20. Suber L, Fiorani D, Imperatori P, Foglia S, Montone A, Zysler R. Effects of thermal treatments on structural and magnetic properties of acicular α-Fe2O3 nanoparticles. NanoStructured Materials. 1999;11(6):797-803.
21. Reddy CG, Seela KK, Manorama S. Preparation of γ-Fe_2O_3 by the hydrazine method: Application as an alcohol sensor. International Journal of Inorganic Materials. 2000; 2(4): 301-7.
22. Jing Z, Wu S, Zhang S, Huang W. Hydrothermal fabrication of various morphological α-Fe2O3 nanoparticles modified by surfactants. Materials research bulletin. 2004;39(13):2057-64.
23. Moradnia F, Ramazani A, Taghavi Fardood S, Gouranlou F. A novel green synthesis and characterization of tetragonal-spinel MgMn2O4 nanoparticles by tragacanth gel and studies of its photocatalytic activity for degradation of reactive blue 21 dye under visible light. Materials Research Express. 2019;6(7):075057.
24. Habibi MH. Synthesis, characterization and photocatalytic properties of Iron oxide nanoparticles synthesized by sol-gel autocombustion with ultrasonic irradiation. Nanochemistry Research. 2017; 2(2): 166-71.
25. Atrak K, Ramazani A, Taghavi Fardood S. A novel sol–gel synthesis and characterization of MgFe2O4@ γ–Al2O3 magnetic nanoparticles using tragacanth gel and its application as a magnetically separable photocatalyst for degradation of organic dyes under visible light. Journal of Materials Science: Materials in Electronics. 2018;29(8):6702-10.
26. Taghavi Fardood S, Moradnia F, Mostafaei M, Afshari Z, Faramarzi V, Ganjkhanlu S. Biosynthesis of $MgFe_2O_4$ magnetic nanoparticles and its application in photo-degradation of malachite green dye and kinetic study. Nanochemistry Research. 2019; 4(1): 86-93.
27. Taghavi Fardood S, Ramazani A, Moradnia F, Afshari Z, Ganjkhanlu S, Yekke Zare F. Green Synthesis of ZnO Nanoparticles via Sol-gel Method and Investigation of Its Application in Solvent-free Synthesis of 12-Aryl-tetrahydrobenzo[α]xanthene-11-one Derivatives Under Microwave Irradiation. Chemical Methodologies. 2019; 3(Issue 6. pp. 684-795): 696-706.
28. Atrak K, Ramazani A, Taghavi Fardood S. Eco-friendly synthesis of Mg0.5Ni0.5AlxFe2-xO4 magnetic nanoparticles and study of their photocatalytic activity for degradation of direct blue 129 dye. Journal of Photochemistry and Photobiology A: Chemistry. 2019;382:111942.
29. Ouni L, Ramazani A, Taghavi Fardood S. An overview of carbon nanotubes role in heavy metals removal from wastewater. Frontiers of Chemical Science and Engineering. 2019;13(2):274–95.
30. Moradi S, Taghavi Fardood S, Ramazani A. Green synthesis and characterization of magnetic NiFe2O4@ ZnO nanocomposite and its application for photocatalytic degradation of organic dyes. Journal of Materials Science: Materials in Electronics. 2018;29(16):14151-60.
31. Amini M, Ashrafi M. Photocatalytic degradation of some organic dyes under solar light irradiation using TiO_2 and ZnO nanoparticles. Nanochemistry Research. 2016; 1(1): 79-86.
32. Taghavi Fardood S, Moradnia F, Ramazani A. Green synthesis and characterisation of ZnMn2O4 nanoparticles for photocatalytic degradation of Congo red dye and kinetic study. Micro & Nano Letters. 2019;14(9):986-91.
33. Zhao B, Wang Y, Guo H, Wang J, He Y, Jiao Z, et al.

Iron oxide(III) nanoparticles fabricated by electron beam irradiation method. Materials Science Poland. 2007; 25(4): 1143-8.
34. Taghavi Fardood S, Ramazani A, Joo SW. Eco-friendly synthesis of magnesium oxide nanoparticles using arabic Gum. Journal of Applied Chemical Research. 2018; 12(1): 8-15.
35. Nouri J, Khoshravesh T, Khanahmadzadeh S, Salehabadi A, Enhessari M. Synthesis, characterization and optical band gap of Lithium cathode materials: $Li_2Ni_8O_{10}$ and $LiMn_2O_4$ nanoparticles. International Journal of Nano Dimension. 2016; 7(1): 15-24.